

# Wave energy Part 2

## Wave energy absorption

OCEN4007 Ocean Renewable Energy

Adi Kurniawan  
[adi.kurniawan@uwa.edu.au](mailto:adi.kurniawan@uwa.edu.au)

In Part 1, we started by looking at some of the advantages of wave energy and a brief history of the field. We then looked at the wave energy resource, where we considered briefly how ocean waves are generated, how to calculate the power transported by regular and irregular waves, how to calculate the mean wave-power level at a given site, and where we also considered the global distribution of wave-power resource and its variability. In passing, we also looked at the group velocity and the role it plays in wave energy propagation. In this part, we will mainly consider the fundamental principles of wave energy absorption.

### 1 A simple oscillator

Wave energy converters (WECs) come in a variety of forms, but most of them are similar in principle. With the exception of overtopping devices, most WECs can be categorised as either *oscillating bodies* or *oscillating water columns*. The keyword here is oscillation. Oscillating bodies utilise motion relative to the sea bed or other bodies. Oscillating water columns utilise motion of water relative to a fixed or moving chamber (see Fig. 1). These motions are converted into a useful form of energy by a *power take-off (PTO)* unit, which can either be a mechanical, hydraulic,

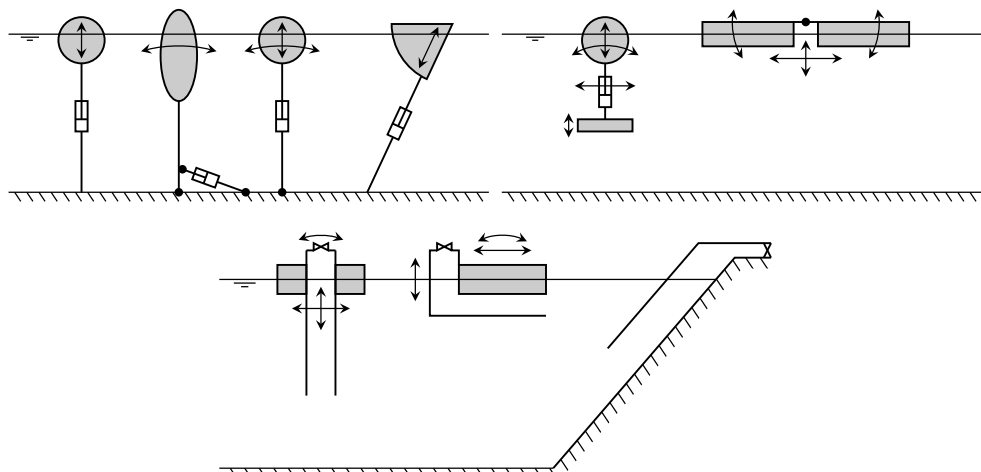


FIGURE 1: Oscillating bodies (top) and oscillating water columns (bottom). Arrows indicate modes of motion.

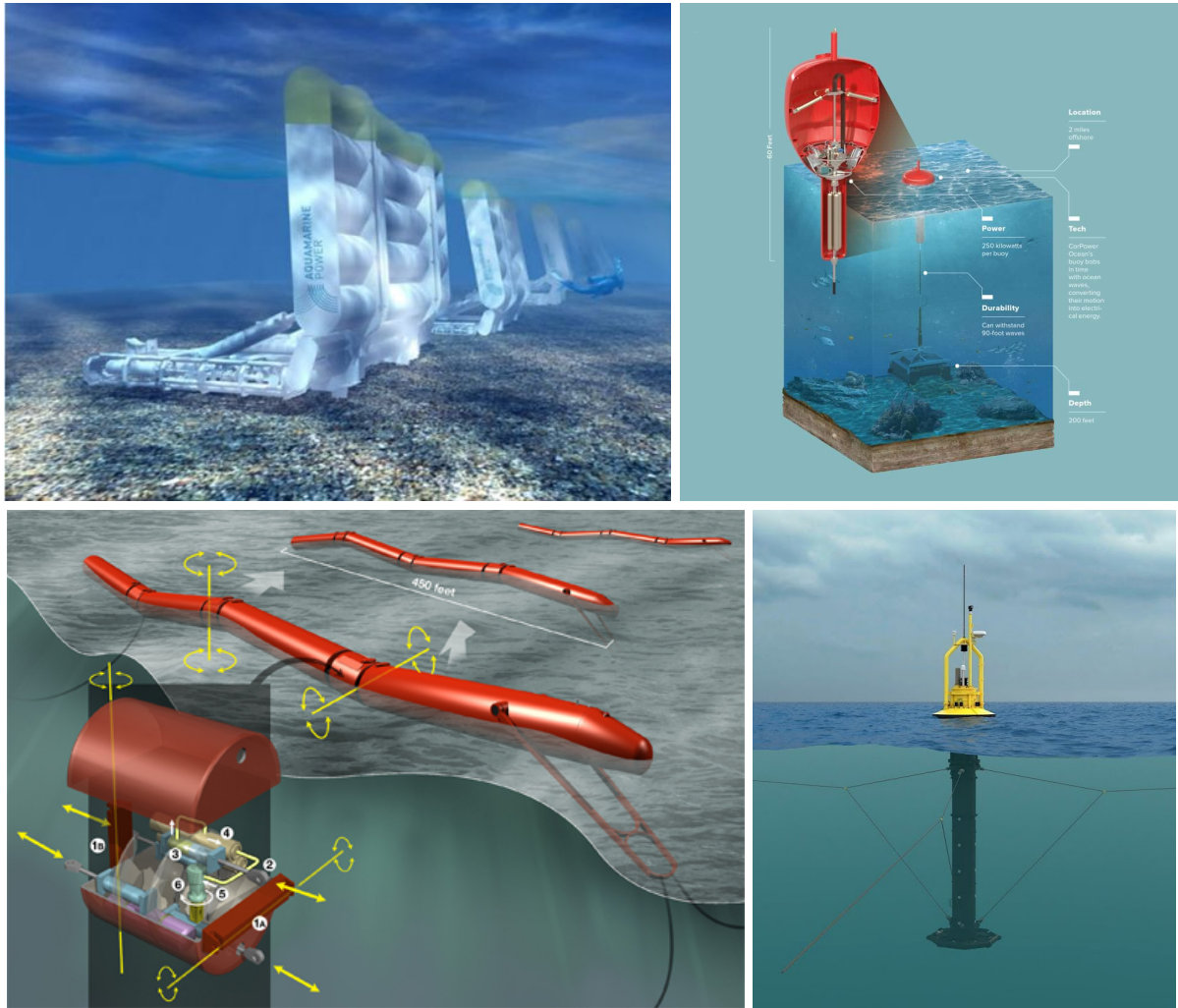


FIGURE 2: Examples of oscillating-body WECs. Clockwise from top left: Oyster, CorPower, OPT Power-Buoy, Pelamis.



FIGURE 3: Example of oscillating-water-column WECs: Limpet OWC.

pneumatic, or a direct drive system. The final product is usually electricity, although other uses are possible, such as desalination. Figs. 2–3 show some examples of oscillating-body and OWC devices that have been deployed in the ocean.

At its core, a WEC is an oscillator in water, driven by the waves. So, before considering how

we can model a realistic WEC, let us first consider a simple oscillator, as shown in Fig. 4. Our aim is to understand the building blocks and the behaviour of a simple oscillator, which will be useful when it comes to understanding the behaviour of a WEC.

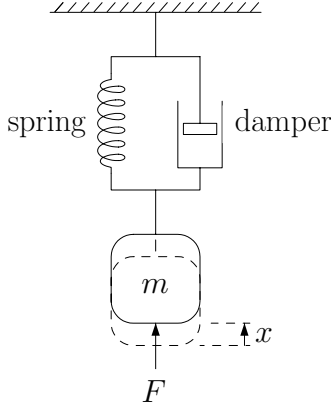


FIGURE 4: A simple oscillator, reproduced from [3].

## 1.1 Equation of motion

The equation of motion of a simple oscillator with a constant mass  $m$ , as in Fig. 4, can be written, according to Newton's second law of motion, as

$$ma = m\ddot{x} = F + F_R + F_S, \quad (1)$$

where  $a$  is the acceleration,  $x$  is the displacement,  $F_R$  is the damping force,  $F_S$  is the spring force, and  $F$  is the excitation force. If the spring and damper have linear characteristics (which we will generally assume in these lectures), we can write

$$F_S = -Sx \quad \text{and} \quad F_R = -Ru = -R\dot{x}, \quad (2)$$

where  $u$  is the velocity,  $S$  and  $R$  are stiffness and damping coefficients. That is, the spring force is linearly proportional to the displacement, while the damping force is proportional to the velocity. Thus,

$$m\ddot{x} + R\dot{x} + Sx = F, \quad (3)$$

which is a second-order linear ordinary differential equation. We are mostly interested in cases where the excitation force  $F$  is a harmonic (sinusoidal) function of time, as in excitation by waves.

## 1.2 Complex amplitudes

A useful tool for analysing harmonic oscillations is the notion of complex amplitudes.

With the use of Euler's formula

$$e^{i\psi} = \cos \psi + i \sin \psi, \quad (4)$$

or, equivalently,

$$\cos \psi = \operatorname{Re}\{e^{i\psi}\} = (e^{i\psi} + e^{-i\psi})/2, \quad (5)$$

$$\sin \psi = \operatorname{Im}\{e^{i\psi}\} = (e^{i\psi} - e^{-i\psi})/2i, \quad (6)$$

a harmonically oscillating quantity with frequency  $\omega$ ,

$$x(t) = x_0 \cos(\omega t + \varphi_x), \quad (7)$$

where  $t$  is time,  $\varphi_x$  is the phase, and  $x_0$  is the amplitude, can be written as

$$\begin{aligned} x(t) &= x_0 \operatorname{Re}\{e^{i(\omega t + \varphi_x)}\} \\ &= \operatorname{Re}\{x_0 e^{i\omega t} e^{i\varphi_x}\}. \end{aligned} \quad (8)$$

Introducing the complex amplitude

$$\hat{x} \equiv x_0 e^{i\varphi_x} \equiv |\hat{x}| e^{i\varphi_x}, \quad (9)$$

we can write (8) as

$$x(t) = x_0 \cos(\omega t + \varphi_x) = \operatorname{Re}\{\hat{x} e^{i\omega t}\}. \quad (10)$$

Furthermore, the first and second time derivative of  $x(t)$  can be written as

$$u \equiv \dot{x} \equiv \frac{dx}{dt} = \operatorname{Re}\{i\omega \hat{x} e^{i\omega t}\}, \quad (11)$$

$$a \equiv \ddot{x} \equiv \frac{du}{dt} \equiv \frac{d^2x}{dt^2} = \operatorname{Re}\{-\omega^2 \hat{x} e^{i\omega t}\}. \quad (12)$$

Writing  $u(t)$  in terms of the complex amplitude  $\hat{x}$ , and  $a(t)$  in terms of the complex amplitude  $\hat{x}$ , we therefore have  $\hat{u} = i\omega \hat{x}$  and  $\hat{a} = i\omega \hat{u} = -\omega^2 \hat{x}$ . Thus, to differentiate a harmonically oscillating quantity with respect to time is equivalent to multiplying its complex amplitude by  $i\omega$ .

The complex amplitude (9) can be represented as a vector in the complex plane (see Fig. 5). The amplitude  $x_0 = |\hat{x}|$  is the modulus of the vector, while the phase  $\varphi_x$  is the angle between the vector and the real axis.

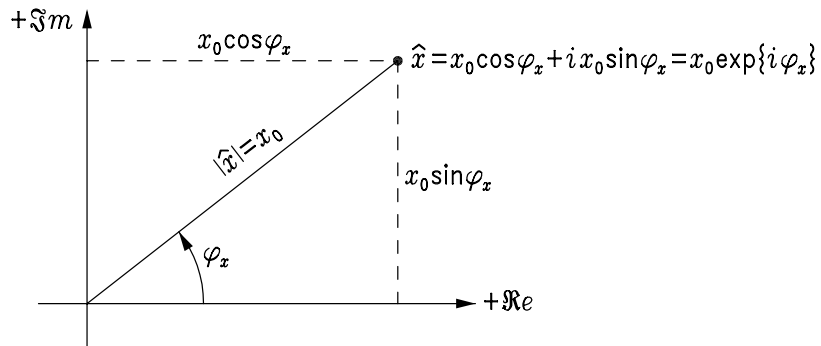


FIGURE 5: A complex amplitude  $\hat{x}$  contains information about the amplitude  $x_0 = |\hat{x}|$  and the phase  $\varphi_x$  of the oscillating quantity  $x(t)$ . Reproduced from [3].

From

$$\hat{u} = i\omega \hat{x} \quad (13)$$

and making use of the identity  $i = e^{i\pi/2}$ , we also have

$$u_0 e^{i\varphi_u} = i\omega x_0 e^{i\varphi_x} = \omega x_0 e^{i(\varphi_x + \pi/2)}, \quad (14)$$

which gives

$$u_0 = \omega x_0 \quad \text{and} \quad \varphi_u = \varphi_x + \pi/2. \quad (15)$$

Similarly,

$$a_0 = \omega u_0 = \omega^2 x_0 \quad \text{and} \quad \varphi_a = \varphi_u + \pi/2 = \varphi_x + \pi. \quad (16)$$

From the phase relationships, we see that displacement lags velocity by  $\pi/2$ , whereas acceleration leads velocity by  $\pi/2$ .

### 1.3 Impedance and reactance

Returning to the simple oscillator, if the excitation force is harmonically varying with an angular frequency  $\omega$ , i.e., if  $F(t)$  is of the form

$$F(t) = F_0 \cos(\omega t + \varphi_F) = \operatorname{Re}\{F_0 e^{i\varphi_F} e^{i\omega t}\} = \operatorname{Re}\{\hat{F} e^{i\omega t}\}, \quad (17)$$

then the steady-state response (i.e. the response after the transients have decayed away) will also be harmonically varying and, if the system is linear, will vary with the same frequency  $\omega$ , i.e., it will have the form

$$u(t) = u_0 \cos(\omega t + \varphi_u) = \operatorname{Re}\{u_0 e^{i\varphi_u} e^{i\omega t}\} = \operatorname{Re}\{\hat{u} e^{i\omega t}\}. \quad (18)$$

Substituting (17) and (18) into (3), we have

$$[i\omega m + R + S/(i\omega)]\hat{u} = \hat{F}, \quad (19)$$

after cancelling out the  $e^{i\omega t}$  from both sides of the equation. Note that  $\hat{u}$  and  $\hat{F}$  are complex, whereas  $m$ ,  $R$ , and  $S$  are real. This equation, which describes the simple harmonic motion of an oscillator, is the basic equation to describe the dynamics of many oscillating systems, including a wave energy converter.

We can write (19) more compactly as

$$Z\hat{u} = \hat{F}, \quad (20)$$

if we introduce the *impedance*  $Z$ , defined as

$$Z = R + i(\omega m - S/\omega) = R + iX, \quad (21)$$

where the imaginary part  $X$  of the impedance is called the *reactance*.

Note that  $m$ ,  $R$ , and  $S$  are known parameters of the system. Thus, for a given  $\hat{F}$ , we can solve (20) for  $\hat{u}$ .

## 1.4 Resonance

We can see from (21) that  $X = 0$  when

$$\omega = \omega_0 = \sqrt{S/m}. \quad (22)$$

This is the *resonance* frequency. At this frequency, we have  $Z = R$  and the velocity response amplitude,  $|\hat{u}/\hat{F}|$ , is maximum:

$$|\hat{u}/\hat{F}|_{\max} = (u_0/F_0)_{\max} = 1/|Z|_{\min} = 1/R. \quad (23)$$

## 1.5 Frequency response function

Looking at (19), we can observe that

1. At the resonance frequency  $\omega = \omega_0$ , the reactance cancels ( $X = 0$ ), and so  $F = Ru$ , i.e., the velocity is in phase with the excitation force (since  $R$  is real) and  $u_0/F_0 = 1/R$ .
2. At  $\omega \ll \omega_0$ , the stiffness term dominates, i.e.  $F \rightarrow Sx$ , or the displacement is in phase with the excitation force (since  $S$  is real) and  $u_0/F_0 = \omega/S$  (cf. (15)).
3. At  $\omega \gg \omega_0$ , the inertial term dominates, i.e.  $F \rightarrow ma$ , or the acceleration is in phase with the excitation force (since  $m$  is real) and  $u_0/F_0 = 1/\omega m$  (cf. (16)).

These explain why the (normalised) frequency response functions of the velocity amplitude and phase (relative to the phase of the excitation force) look like those in Fig. 6. At resonance, or  $\omega\sqrt{m/S} = 1$ , the velocity amplitude is maximum and in phase with the excitation force (hence  $\varphi_u - \varphi_F = 0$ ). At  $\omega \ll \omega_0$  (or  $\omega\sqrt{m/S} \ll 1$ ), the slope of the curve in Fig. 6a is 1, because  $|\hat{u}/\hat{F}| = \omega/S$ , whereas at  $\omega \gg \omega_0$  (or  $\omega\sqrt{m/S} \gg 1$ ), the slope of the curve is  $-1$ , because  $|\hat{u}/\hat{F}| = 1/\omega m$ . At  $\omega \ll \omega_0$ , the displacement is in phase with the excitation force, and so the velocity leads the force by  $\pi/2$ . At  $\omega \gg \omega_0$ , the acceleration is in phase with the excitation force, and so the velocity lags the force by  $\pi/2$ .

As an exercise, try replotting Fig. 6 in linear scale instead of log scale!

## 1.6 Delivered power and consumed power

The *delivered* power  $P(t)$  is the power delivered by the excitation force into the system. Recall that power is force times velocity. So,

$$\begin{aligned} P(t) &= F(t)u(t) = \operatorname{Re}\{\hat{F}e^{i\omega t}\}\operatorname{Re}\{\hat{u}e^{i\omega t}\} \\ &= \frac{1}{2}(\hat{F}e^{i\omega t} + \hat{F}^*e^{-i\omega t})\frac{1}{2}(\hat{u}e^{i\omega t} + \hat{u}^*e^{-i\omega t}) \\ &= \frac{1}{4}(\hat{F}\hat{u}^* + \hat{F}^*\hat{u} + \hat{F}\hat{u}e^{2i\omega t} + \hat{F}^*\hat{u}^*e^{-2i\omega t}) \\ &= \frac{1}{2}\operatorname{Re}\{\hat{F}\hat{u}^*\} + \frac{1}{2}\operatorname{Re}\{\hat{F}\hat{u}e^{2i\omega t}\}, \end{aligned} \quad (24)$$

where  $*$  denotes the complex conjugate. The second term is a harmonic oscillation with angular frequency  $2\omega$  and so has a zero time average. Hence, the time-average delivered power is

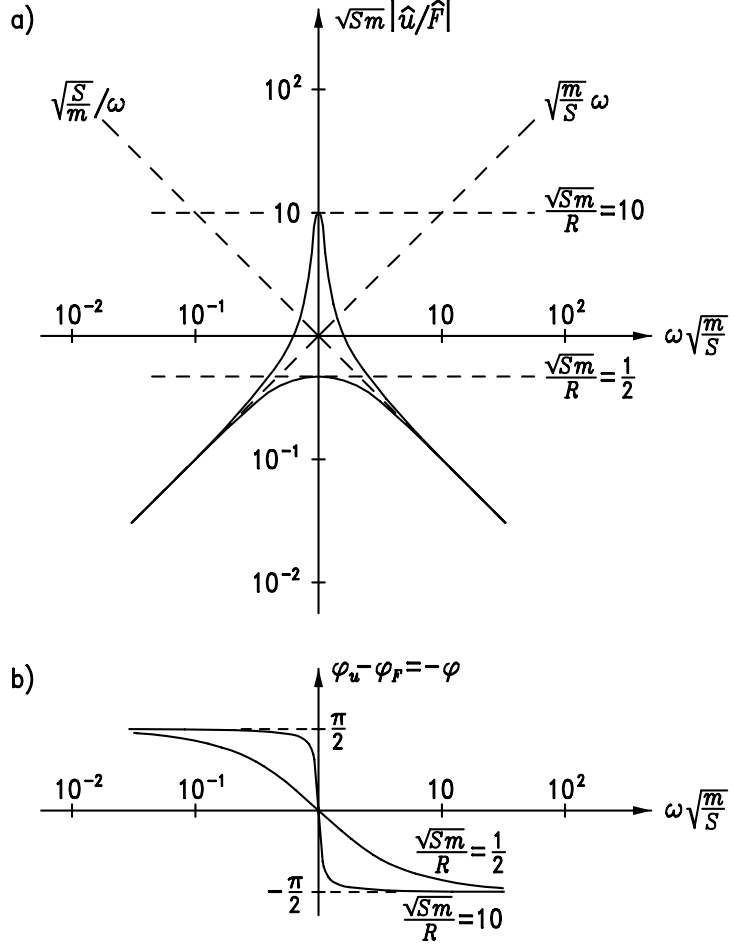


FIGURE 6: Frequency response functions of the (a) velocity amplitude and (b) phase, for two different damping coefficients  $R$ . Reproduced from [3].

$$P \equiv \overline{P(t)} = \frac{1}{2} \operatorname{Re}\{\hat{F}\hat{u}^*\} = \frac{1}{2} \operatorname{Re}\{\hat{Z}\hat{u}\hat{u}^*\} = \frac{1}{2} \operatorname{Re}\{\hat{Z}|\hat{u}|^2\} = \frac{1}{2} R |\hat{u}|^2. \quad (25)$$

The *consumed* power  $P_R(t)$  is the power consumed by the damper:

$$\begin{aligned} P_R(t) &= -F_R(t)u(t) = Ru^2(t) = R \operatorname{Re}\{\hat{u}e^{i\omega t}\} \operatorname{Re}\{\hat{u}e^{i\omega t}\} \\ &= \frac{1}{4}R(\hat{u}e^{i\omega t} + \hat{u}^*e^{-i\omega t})^2 \\ &= \frac{1}{4}R(2\hat{u}\hat{u}^* + \hat{u}^2e^{2i\omega t} + \hat{u}^{*2}e^{-2i\omega t}) \\ &= \frac{1}{2}R|\hat{u}|^2 + \frac{1}{2}\operatorname{Re}\{R\hat{u}^2e^{2i\omega t}\}. \end{aligned} \quad (26)$$

Again, the second term has a zero time average. Hence, the time-average consumed power is  $\frac{1}{2}R|\hat{u}|^2$ .

We see that the consumed power and the delivered power are equal in time average. This will be useful when we consider the (time-average) power absorbed by a WEC in section 4.2.

## 2 An oscillator in water

As a further step towards modelling a WEC, let us put our oscillator in water (see Fig. 7). This can be regarded as a simple WEC oscillating in a single mode (heave). Power is absorbed by the damper—this is our power take-off (PTO).

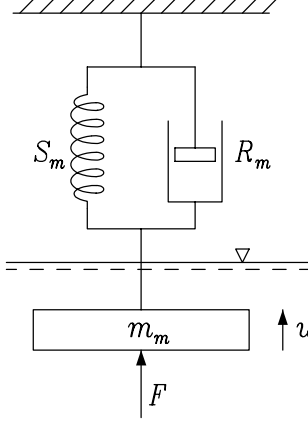


FIGURE 7: An oscillator in water, reproduced from [3].

Let  $F(t) = \text{Re}\{\hat{F}e^{i\omega t}\}$ . Assume a linear system. Thus,  $u(t) = \text{Re}\{\hat{u}e^{i\omega t}\}$ . The (time-average) power consumed by the mechanical damper (our PTO) is

$$P_m = \frac{1}{2}R_m|\hat{u}|^2. \quad (27)$$

### 2.1 Radiation impedance

By analogy with (27), as the body oscillates in the water, it generates a wave which carries away *radiated power*

$$P_r = \frac{1}{2}R_r|\hat{u}|^2, \quad (28)$$

which defines the *radiation damping*  $R_r$ . Due to the radiated wave, a force  $F_r$  acts on the body. Assuming a linear system,  $F_r$  is also harmonically varying, i.e.

$$F_r(t) = \text{Re}\{\hat{F}_r e^{i\omega t}\}. \quad (29)$$

Writing

$$\hat{F}_r = -Z_r \hat{u}, \quad (30)$$

we define the *radiation impedance*  $Z_r$ .

In general,  $Z_r$  is a complex function of frequency, where the real part, in agreement with (28), is the radiation damping:

$$\begin{aligned} Z_r &= Z_r(\omega) = R_r(\omega) + iX_r(\omega) \\ &= R_r(\omega) + i\omega m_r(\omega). \end{aligned} \quad (31)$$

The imaginary part,  $X_r$ , is called the *radiation reactance* and is conventionally written in terms of the *added mass*  $m_r$ . Note that in certain cases the added mass can be negative. The radiation impedance  $Z_r$  depends on the geometry of the radiating system. By geometry we mean the shape of the body and its mode of motion.

As an example, Fig. 8 shows the added mass and radiation damping of the geometry in Fig. 9. At  $\omega \rightarrow 0$  or  $\omega \rightarrow \infty$ , an oscillating body generates no waves; so  $R_r \rightarrow 0$  at these limits.

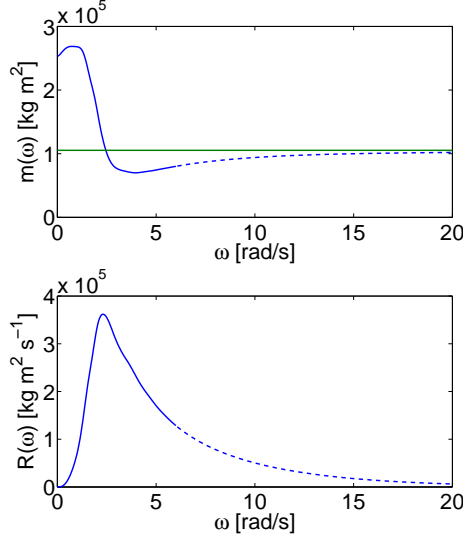


FIGURE 8: Added mass (top) and radiation damping (bottom) of the geometry in Fig. 9 calculated numerically using a boundary element method (BEM)-based code [11], reproduced from [6].

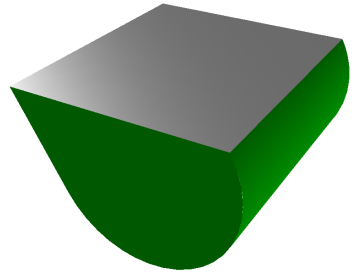


FIGURE 9: Geometry corresponding to the added mass and radiation damping in Fig. 8, reproduced from [6]. The geometry resembles the Salter Duck. It oscillates about a horizontal axis passing through the body. Only the shape below the water surface is shown.

## 2.2 Wave excitation force

So far we have assumed the excitation force  $F$  to be a general excitation force that can be applied e.g. by a mechanical actuator. Let us now assume that the excitation force  $F$  is due to waves incident on the body. In other words, let us consider a true WEC subjected to incident waves and absorbing energy from the waves.

Linear theory allows us to treat the problem of a body oscillating in response to incident waves, as a superposition of two sub-problems (see Fig. 10):

- *diffraction* problem

The body is fixed (not moving) and is subjected to incident waves.

- *radiation* problem

The body is oscillating with an unknown amplitude and phase, in otherwise still water (only waves radiated by the oscillating body are present).

The total hydrodynamic force  $F_t$  on the body is a superposition of the *wave excitation force*  $F_e$  and the *wave radiation force*  $F_r$ , where each is the force due to the wave acting on the body in each of the above problems:

$$F_t = F_e + F_r. \quad (32)$$

Note that  $F_r$  here is none other than the  $F_r$  discussed in section 2.1.

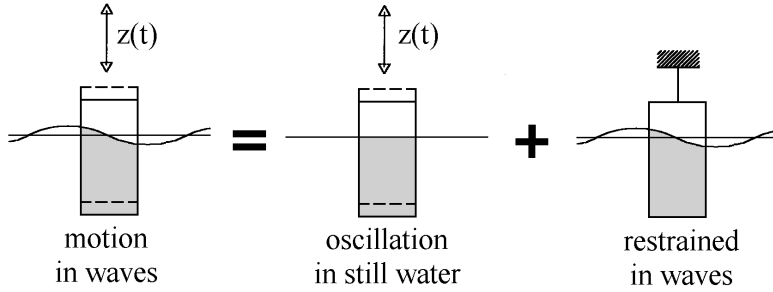


FIGURE 10: The problem of a body oscillating in response to incident waves is, according to linear theory, a superposition of radiation and diffraction problems. Reproduced from [5].

Like  $\hat{F}_r$ , the wave excitation force  $\hat{F}_e$  is also a complex function of frequency. In linear theory,  $\hat{F}_e$  is proportional to the incident wave amplitude  $A$ :

$$\hat{F}_e(\omega) = \hat{f}_e(\omega)A, \quad (33)$$

where  $\hat{f}_e(\omega)$  is defined as the excitation force coefficient. Note that  $A$  here is used to denote the complex incident wave amplitude ( $A$  is real in Part 1).

### 2.3 Equation of motion

With incident wave, in reference to Fig. 7, we now have the following equation describing the motion of the oscillator (cf. (19)):

$$[\mathrm{i}\omega m_m + R_m + S_m/(\mathrm{i}\omega)]\hat{u} = \hat{F}_e + \hat{F}_r, \quad (34)$$

which, upon substituting (30) and defining

$$Z_m \equiv \mathrm{i}\omega m_m + R_m + S_m/(\mathrm{i}\omega), \quad (35)$$

becomes

$$\begin{aligned} Z_m \hat{u} &= \hat{F}_e - Z_r \hat{u} \\ (Z_m + Z_r) \hat{u} &= \hat{F}_e. \end{aligned} \quad (36)$$

In this form, we have rearranged the terms such that only the excitation force appears on the right-hand side. We have defined two impedances: the *mechanical impedance*  $Z_m$  and the radiation impedance  $Z_r$ .

We can solve this equation for the velocity:

$$\begin{aligned} \hat{u} &= \frac{\hat{F}_e}{Z_m + Z_r} \\ &= \frac{\hat{F}_e}{R_m + R_r + \mathrm{i}[\omega(m_m + m_r) - S_m/\omega]}, \end{aligned} \quad (37)$$

where the last equality follows from (35) and (31).

### 3 Absorbed power

#### 3.1 Optimum phase and optimum amplitude conditions

Knowing the velocity  $\hat{u}$ , we can calculate the absorbed power. The time-average power absorbed in the mechanical damper is

$$P_a = \frac{R_m}{2} |\hat{u}|^2 = \frac{(R_m/2) |\hat{F}_e|^2}{(R_m + R_r)^2 + [\omega(m_m + m_r) - S_m/\omega]^2}. \quad (38)$$

Observe that  $P_a = 0$  for  $R_m = 0$  (no PTO damping). Also,  $P_a = 0$  for  $R_m = \infty$  (infinite PTO damping). Somewhere in between, the absorbed power is maximum. To find the value of  $R_m$  that maximises the absorbed power at a given frequency  $\omega$ , we solve  $\frac{\partial P_a}{\partial R_m} = 0$ , which gives

$$R_{m,\text{opt}} = \sqrt{R_r^2 + X^2}, \quad (39)$$

$$P_{a,\text{max}} = \frac{|\hat{F}_e|^2}{4(R_r + R_{m,\text{opt}})}. \quad (40)$$

Here,

$$X = \omega(m_m + m_r) - S_m/\omega \quad (41)$$

is the total reactance. The proof for the above results, (39) and (40), is left as an exercise.

Equation (39) is called the *optimum amplitude condition*, since it specifies how much damping is required to give the optimum motion amplitude that maximises the absorbed power at any given frequency (when the phase is not necessarily optimum—more on this shortly).

Further, if  $X = 0$  (resonance, see section 1.4), then the absorbed power (40) is maximised and is equal to

$$P_{a,\text{MAX}} = \frac{|\hat{F}_e|^2}{8R_r}. \quad (42)$$

The optimum PTO damping is

$$R_{m,\text{OPT}} = R_r, \quad (43)$$

and the optimum velocity is

$$\hat{u}_{\text{OPT}} = \frac{\hat{F}_e}{2R_r}, \quad (44)$$

obtained by substituting  $X = 0$  and  $R_m = R_{m,\text{OPT}} = R_r$  into (37).

We call  $X = 0$  the *optimum phase condition*. When the body oscillates with the velocity as given by (44), it satisfies both the optimum amplitude and the optimum phase conditions.  $P_{a,\text{MAX}}$  as given by (42) is the ultimate maximum absorbed power than can possibly be absorbed by the oscillator from the waves (provided it can realise the optimum motion as given by (44)).  $P_{a,\text{max}}$  as given by (40) is less than or equal to  $P_{a,\text{MAX}}$ .

Observe from (42) that  $P_{a,\text{MAX}}$  is purely a function of the wave excitation force  $\hat{F}_e$  and the radiation damping  $R_r$ . In other words, the maximum possible power that can be absorbed from the wave is governed by the hydrodynamic properties of the body, provided it is possible to realise the optimum motion. Since  $\hat{F}_e$  and  $R_r$  depend on the geometry of the system (body size, shape, and mode of motion),  $P_{a,\text{MAX}}$  also depends on the geometry of the system. Note that since  $\hat{F}_e$  and  $R_r$  vary with frequency, the maximum absorbed power  $P_{a,\text{MAX}}$  and the required optimum motion  $\hat{u}_{\text{OPT}}$  also vary with frequency. This highlights the importance of *bandwidth*, since real ocean waves consist of multiple frequency components.

As an example, Fig. 11 shows the absorbed power of two oscillators as a function of frequency, when the incident wave amplitude is 0.5 m. The two oscillators are made of the same body, i.e. a circular cylinder, but oriented differently and oscillating in different modes. The one at the top is oriented vertically and is oscillating in heave (vertical direction). The one at the bottom is oriented horizontally and is oscillating about a hinge at the seabed. However, the two oscillators are tuned to have the same resonance frequency  $\omega_0 = 0.9 \text{ rad/s}$ . In each plot there are three lines: the solid black line is the maximum absorbed power  $P_{a,\text{MAX}}$  as given by (42); the dashed blue line and the dash-dotted red line are both the absorbed power  $P_a$  as obtained from (38) with constant  $R_m$ , but the dashed blue line is obtained with  $R_m = R_r(\omega_0)$ , whereas the dash-dotted red line is obtained with  $R_m$  greater than  $R_r(\omega_0)$ .

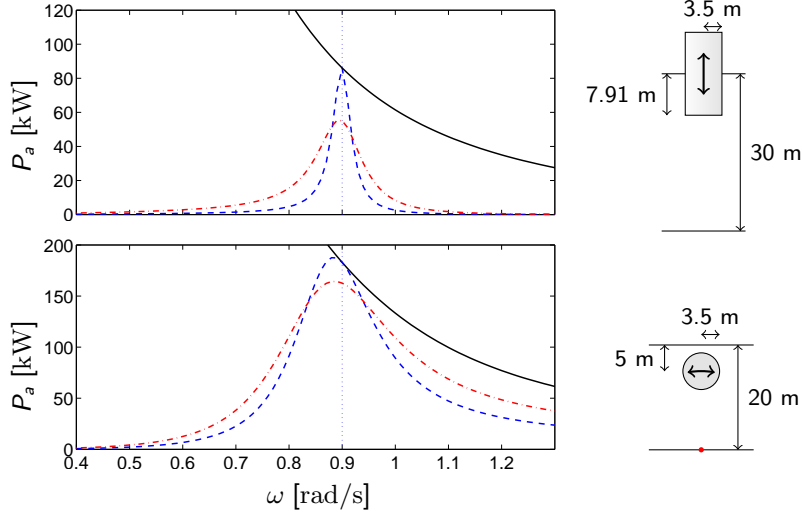


FIGURE 11: Power absorption characteristics of two oscillators. Solid line: maximum absorbed power  $P_{a,\text{MAX}}$ ; dashed and dash-dotted lines: absorbed power  $P_a$  for different mechanical damping  $R_m$  values. The blue dashed lines are obtained with  $R_m = R_r(\omega_0)$ , whereas the red dash-dotted lines are obtained with  $R_m > R_r(\omega_0)$ . Adapted from [8].

Observe how the absorbed power  $P_a$  varies with frequency  $\omega$ , and that  $P_a = P_{a,\text{MAX}}$  when both  $X = 0$  and  $R_m = R_r$  (as shown by the blue dashed lines touching the black solid lines at  $\omega = \omega_0 = 0.9 \text{ rad/s}$ ). If either of these conditions is not met, then  $P_a(\omega) < P_{a,\text{MAX}}(\omega)$ . For example, the blue dashed lines are not touching the black solid lines away from  $\omega_0$ , because at least the phase condition is not met, since  $X \neq 0$  for  $\omega \neq \omega_0$ . Likewise, the red dash-dotted lines are not touching the black solid lines even at  $\omega = \omega_0$ , because  $R_m \neq R_r(\omega_0)$  in this case.

Notice that the power absorption capacity is approximately doubled when the cylinder is oscillating horizontally instead of vertically. Likewise, the bandwidth (the broadness of the curve) of the

absorbed power  $P_a$  is broader for the horizontal cylinder. In addition, increasing the mechanical damping  $R_m$  reduces the peak of the curve but broadens the bandwidth.

In reality,  $P_a$  is also limited by losses and practical constraints, which we will discuss later.

### 3.2 Capture width (absorption width)

The power performance of a WEC is normally expressed in terms of its *capture width*, defined as the ratio between the absorbed power and the wave-power level:

$$d_a \equiv \frac{P_a}{J}. \quad (45)$$

This can be understood as the width of the wave front carrying the same amount of energy as that absorbed by the WEC. The capture width can be expressed in terms of the incident wavelength  $\lambda$ , as we will show later. For some simple geometries, simple expressions for the maximum capture width exist, such as

$$d_{a,\text{MAX}} = \frac{\lambda}{2\pi} \text{ for a heaving axisymmetric body.} \quad (46)$$

Notice that (46) does not depend on the size of the WEC!

**Example** A WEC in the form of a vertical circular cylinder is absorbing wave energy through its vertical motion. What is its maximum capture width in regular wave of period 8 s and amplitude 1 m? Theoretically, how much power can it potentially absorb from this wave? Assume deep water condition.

**Answer** The expression for a heaving axisymmetric body,  $d_{a,\text{MAX}} = \frac{\lambda}{2\pi}$ , applies. The wavelength for  $T = 8$  s, assuming deep water condition, is (from deep-water dispersion equation)

$$\lambda = \frac{gT^2}{2\pi} = \frac{9.81 \times 8^2}{2\pi} \approx 100 \text{ m.}$$

Thus,

$$d_{a,\text{MAX}} = \frac{\lambda}{2\pi} \approx \frac{100}{2\pi} \approx 16 \text{ m.}$$

The wave-power level available in the (deep-water) regular waves is approximately

$$J \approx TH^2 = 8 \times 2^2 = 32 \text{ kW/m.}$$

The maximum power that it can potentially absorb is therefore

$$P_{a,\text{MAX}} = d_{a,\text{MAX}} J \approx 16 \times 32 \approx 500 \text{ kW.}$$

### 3.3 Capture width ratio

Dividing the capture width by the frontal width of the WEC, we get a nondimensional quantity often referred to as the *capture width ratio*:

$$\text{CWR} = \frac{d_a}{D}, \quad (47)$$

where  $D$  is the width of the WEC. Sometimes this quantity is called ‘efficiency’, but note that its value can be greater than unity, making it inappropriate to call it efficiency.

## 4 Principles of wave energy absorption

### 4.1 Wave absorption as destructive interference

One key principle of wave energy absorption (by oscillating systems) is that *to absorb a wave is to generate a wave*.

To illustrate this, consider a wave flume terminating with a rigid wall at the end, as in Fig. 12. The incident wave propagates from left to right. The incoming energy is proportional to the square of the incident wave amplitude. If the wall is completely rigid, the wave will be totally reflected, so the reflected wave amplitude is equal to the incident wave amplitude. The outgoing energy is therefore equal to the incoming energy. The energy absorbed by the wall, which is given by the difference between the incoming energy and the outgoing energy, is zero in this case.

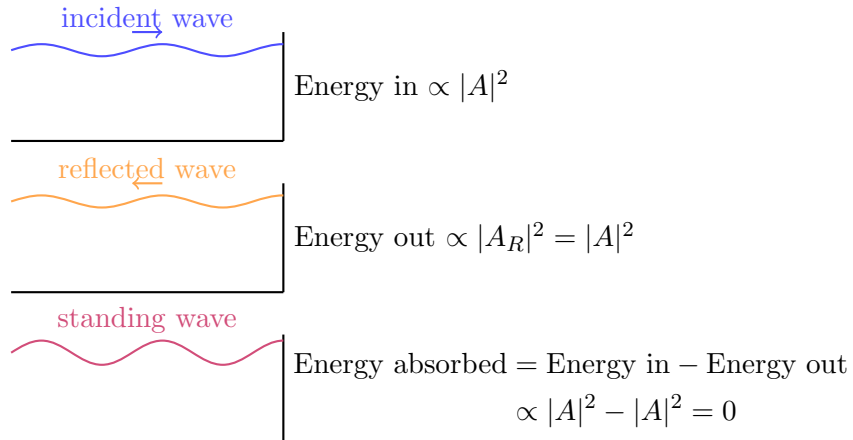


FIGURE 12: Incident wave reflected by a rigid wall, resulting in a standing wave.

Let us now allow the wall to oscillate about a hinge at the bottom, as in Fig. 13. Again, the incident wave will be diffracted by the wall, but in this case, the oscillation of the wall radiates a wave that also propagates to the left (cf. section 2.2). If the wall is made to oscillate in such a way that the radiated wave cancels out the diffracted wave, then the outgoing energy is zero. The energy absorbed by the wall is therefore equal to the incoming energy. In other words, the incident wave energy is completely absorbed by the wall. This is possible only because the wall is generating a wave. The oscillating wall becomes a perfect wave absorber provided it can generate a wave of the right amplitude and phase to cancel out the diffracted wave. This illustrates the

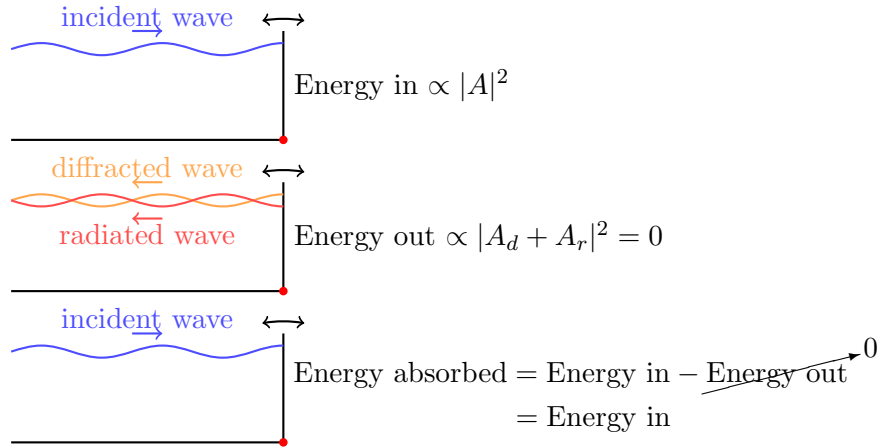


FIGURE 13: The incident wave is completely absorbed if the wall generates radiated wave that cancels out the diffracted wave. This requires the phase and amplitude of the motion to be optimal.

optimum amplitude and optimum phase conditions for maximum power absorption discussed in section 3.1.

Moving on to a more realistic case, let us consider a WEC in a flume, where there is water to the left as well as to the right of the WEC, as in Fig. 14. In this case, we need to take into account both sides of the WEC. The incident wave again propagates from left to right. The incoming energy from the left is proportional to the square of the incident wave amplitude. The incoming energy from the right is zero, since there is no wave coming from the right. The outgoing wave from the WEC to the left is the sum of the diffracted wave and radiated wave going to the left,  $A_d^- + A_r^-$ .

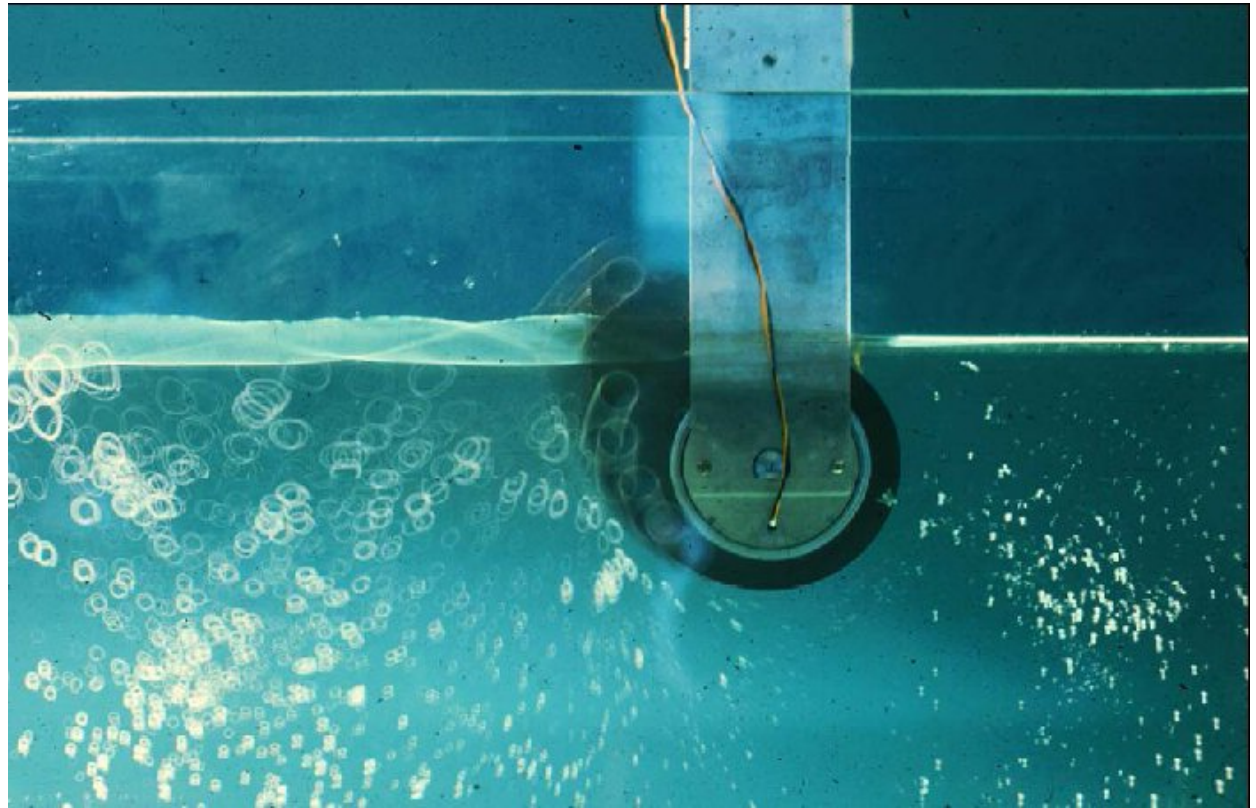


FIGURE 14: Salter Duck in a wave flume. Incident waves propagate from left to right. Reproduced from [10].

The outgoing wave from the WEC to the right is the sum of the diffracted and radiated waves going to the right plus the incident wave,  $A_d^+ + A_r^+ + A$ . The absorbed energy is therefore proportional to  $|A|^2 - |A_d^- + A_r^-|^2 - |A + A_d^+ + A_r^+|^2$ . From here it is clear that since the second and third terms are always positive, perfect absorption is only possible if the WEC radiates waves that cancel out the diffracted wave going to the left and the sum of the incident and diffracted waves going to the right.

**Example** Fig. 14 shows a 1-second exposure photograph of a scaled model of the Salter Duck in a wave flume. The Duck spans the width of the flume. Estimate the proportion of the incident wave energy being absorbed by the Duck.

**Answer** The thick band on the left indicates that  $|A_d^- + A_r^-| \ll |A|$  (waves going to the left is much smaller than the incident wave). This we can tell by observing the depth of the kinks in the band (which gives the height of the outgoing wave to the left) relative to the average thickness of the band (which gives the height of the incident wave). This appears to be about 1/5. In addition, the thin band on the right indicates that  $|A + A_d^+ + A_r^+| \approx 0$  (waves going to the right is almost zero). Since wave energy is proportional to the height (or amplitude) squared, this means that 1/25 or 4% of the incoming energy is going to the left and, therefore, 100% - 4% - 0% = 96% of the incident wave energy is being absorbed by the Duck.

For a WEC in the open sea, the principle still stands. Absorbing wave energy means that energy has to be removed from the waves. Hence, there must be a cancellation or reduction of waves which pass a WEC or are reflected from it. Such cancellation or reduction of waves can be realised by the oscillating WEC, provided it generates waves which oppose (are in counterphase with) the passing and/or reflected waves. The task of a WEC is to generate a wave that interferes destructively with the other waves such that if we define a control volume enclosing the WEC, the energy that goes out of the volume is less than the energy that goes into the volume. To maximise this cancellation, the phase and amplitude of the WEC's oscillation have to be optimum.

## 4.2 Absorbed power

The key principle that we have illustrated above, that it is necessary for a WEC to radiate a wave in order to absorb a wave, can be proven mathematically. Consider again a single oscillator (a WEC oscillating in one mode) subjected to incident wave (cf. section 2.3):

$$\begin{aligned} [\mathrm{i}\omega m_m + R_m + S_m/(\mathrm{i}\omega)]\hat{u} &= \hat{F}_e + \hat{F}_r \\ (R_m + \mathrm{i}X_m)\hat{u} &= \hat{F}_e - Z_r\hat{u} \end{aligned} \tag{48}$$

Multiplying each term by  $\hat{u}^*/2$  and taking the real part, we obtain the time-average power (cf. section 1.6):

$$\begin{aligned} \mathrm{Re}\{(R_m + \mathrm{i}X_m)\hat{u}\hat{u}^*/2\} &= \mathrm{Re}\{(\hat{F}_e - Z_r\hat{u})\hat{u}^*/2\} \\ \underbrace{\frac{R_m}{2}|\hat{u}|^2}_{P_a} &= \underbrace{\frac{1}{2}\mathrm{Re}\{\hat{F}_e\hat{u}^*\}}_{P_e} - \underbrace{\frac{R_r}{2}|\hat{u}|^2}_{P_r}. \end{aligned} \tag{49}$$

We can see that the absorbed power  $P_a$  is equal to the excitation power  $P_e$  minus the radiated power  $P_r$ . In other words, the absorbed power can be obtained without knowing the details of the power take-off system. (Remember from section 1.6 that the delivered power and the consumed power are equal in time average.)

The excitation power can be written as

$$\begin{aligned} P_e &= \frac{1}{2} \operatorname{Re}\{\hat{F}_e \hat{u}^*\} \\ &= \frac{1}{2} \operatorname{Re}\{|\hat{F}_e| e^{i\varphi_F} |\hat{u}| e^{-i\varphi_u}\} \\ &= \frac{1}{2} |\hat{F}_e| |\hat{u}| \cos \gamma, \end{aligned} \quad (50)$$

where  $\gamma = \varphi_u - \varphi_F$ , the phase difference between the velocity  $u$  and the excitation force  $F_e$ . (Note that, when the total reactance  $X = 0$  (cf. (41)), we have  $\gamma = 0$  and hence  $\cos \gamma = 1$  and  $P_e = \frac{1}{2} |\hat{F}_e| |\hat{u}|$ .)

From (49)–(50) we see that  $P_e$  is *linear* in  $|\hat{u}|$ , while  $P_r$  is *quadratic* in  $|\hat{u}|$ . Plotting  $P_e$  and  $P_r$  against  $|\hat{u}|$ , we have the plot in Fig. 15.

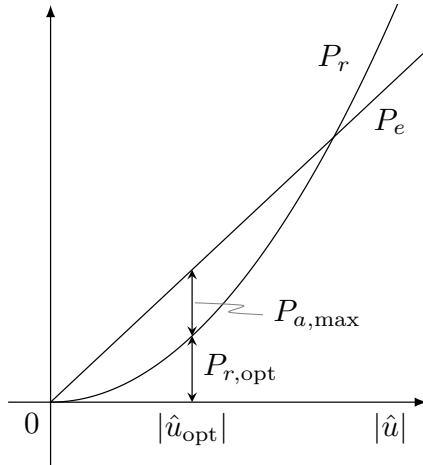


FIGURE 15: The variation of the excitation power  $P_e$  and the radiated power  $P_r$  with the body velocity  $|\hat{u}|$ .

Solving  $\frac{\partial P_a}{\partial |\hat{u}|} = 0$  or inspecting the plot, we find that the absorbed power  $P_a = P_e - P_r$  is maximised when

$$P_{a,\max} = P_{r,\text{opt}} = \frac{1}{2} P_{e,\text{opt}}. \quad (51)$$

(The proof is left as an exercise.) In other words, to maximise power absorption, the WEC has to radiate as much power as it absorbs. Thus, we have shown that it is *necessary* for the WEC to radiate waves in order to absorb any power from the waves. If the WEC does not radiate any waves (such as when it is held fixed), then the absorbed power will be zero. Likewise, if the radiated waves are too large, then the absorbed power will be zero or even negative (power is input into rather than taken out of the waves). Equation (51) is true for any oscillating WEC system, including arrays of multiple WECs. In the latter case, the total maximum absorbed power is equal to the total radiated power.

The optimum velocity amplitude (obtained by solving  $\frac{\partial P_a}{\partial |\hat{u}|} = 0$ ) is

$$|\hat{u}_{\text{opt}}| = \frac{|\hat{F}_e|}{2R_r} \cos \gamma. \quad (52)$$

If, in addition,  $u$  is in phase with  $F_e$ , i.e.  $\gamma = 0$ , then

$$\hat{u} = \hat{u}_{\text{OPT}} = \frac{\hat{F}_e}{2R_r}, \quad (53)$$

which gives

$$P_a = P_{a,\text{MAX}} = \frac{|\hat{F}_e|^2}{8R_r}. \quad (54)$$

Observe that these are the same results as we have seen before, when we solved for the optimum damping  $R_m$  (see (42) and (44)).

Thus, we have shown two routes to the same set of results, one by optimising the power take-off damping  $R_m$ , and the other by optimising the body velocity  $|\hat{u}|$  without caring about the detail of the power take-off.

### 4.3 Far-field theory

There is yet another route to the same result, which is by considering only the far field, without caring about the detail of the WEC (we touched on this briefly at the end of section 4.1). If we imagine a vertical cylinder enclosing all WECs in the system, with a large diameter such that the cylinder wall is sufficiently far from the WECs, such as in Fig. 16, then the absorbed power is the

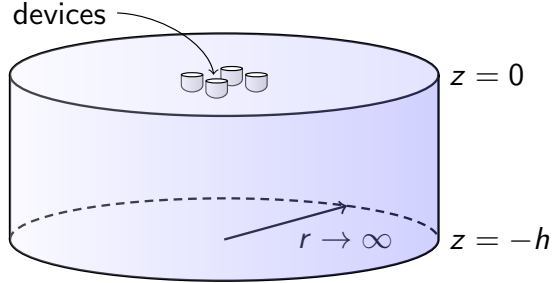


FIGURE 16: An envisaged cylinder containing the WEC system.

net wave power that is transported into the cylinder. Recalling the definition of intensity from Part 1, we find that the absorbed power is the intensity integrated over the surface area of the cylinder:

$$P_a = - \int_{-h}^0 \int_0^{2\pi} \underbrace{\frac{1}{2} \text{Re}\{pv_r^*\}}_{\text{intensity}} r d\theta dz, \quad (55)$$

where  $p$  is the total hydrodynamic pressure and  $v_r$  is the  $r$ -component of the total fluid velocity. The negative sign is because  $r$  is pointing outward, whereas we are interested in the net power *into* the cylinder. The integral is taken only over the vertical surface of the cylinder since there is no

energy transport through the horizontal surfaces (the sea bed and the free surface). Each of  $p$  and  $v_r$  is a sum of three terms associated with the incident, diffracted, and radiated waves. Without going into the details, the maximum mean absorbed power can be shown to be

$$P_{a,\text{MAX}} = \frac{J}{k} G, \quad (56)$$

or, in terms of capture width,

$$d_{a,\text{MAX}} = \frac{G}{k}, \quad (57)$$

Here,  $J$  is the wave-power level,  $k = 2\pi/\lambda$  is the wavenumber, and  $G$  is the *optimum gain function*. The optimum gain function,

$$G = 2\pi \frac{|\bar{H}_{r\text{opt}}(\beta \pm \pi)|^2}{\int_0^{2\pi} |H_{r\text{opt}}(\theta)|^2 d\theta}, \quad (58)$$

where  $\beta$  is the incident wave direction, is related to the far-field pattern of waves radiated by the WEC system when it oscillates optimally, as described by the Kochin functions  $H_{r\text{opt}}(\theta)$  and  $\bar{H}_{r\text{opt}}(\theta)$ . The form of equation (58) tells us that a system capable of radiating waves in one predominant direction has a high  $P_{a,\text{MAX}}$ .

Simple expressions for the optimum gain function exist for simple geometries. For a *monopole* radiator, i.e., a body making a wave radiation pattern as in Fig. 17 (left), for example an axisymmetric body oscillating in heave,

$$G = 1, \quad (59)$$

$$d_{a,\text{MAX}} = \frac{1}{k} = \frac{\lambda}{2\pi}. \quad (60)$$

FIGURE 17: Wave radiation pattern from a monopole (left) and from a dipole (right). Animation courtesy of Dr. Dan Russell, Grad. Prog. Acoustics, Penn State.

For a *dipole* radiator, i.e., a body making a wave radiation pattern as in Fig. 17 (right), for example a small body oscillating in surge or pitch,

$$G = 2, \quad (61)$$

$$d_{a,\text{MAX}} = \frac{2}{k} = \frac{\lambda}{\pi}. \quad (62)$$

In summary, the key principles of wave energy absorption are as follows:

- It is impossible to absorb a wave without radiating a wave (with the exception of overtopping devices).
- Our aim is not to make the WEC respond as much as possible, but respond at the right phase and amplitude. Not only the amplitude but also the phase of the oscillation have to be optimal (easy for regular wave, but challenging for irregular wave).
- A good wave absorber or an array of wave absorbers needs to be good at making waves (into one predominant direction). Note that a good wave absorber is not necessarily a good WEC, because a good WEC not only needs to have a good wave absorption but also needs to do this at minimum cost.
- It is important to have as broad resonance bandwidth as possible. More on this shortly.

#### 4.4 Resonance bandwidth

We have earlier touched upon resonance bandwidth. Because a real sea is composed of many frequency components, it is important for a WEC to have as broad resonance bandwidth as possible. The resonance bandwidth  $\Delta\omega$  is defined as the frequency interval  $\omega_u - \omega_l$  in which the relative absorbed-power response  $\frac{P_a(\omega)/|\hat{F}_e(\omega)|^2}{P_a(\omega_0)/|\hat{F}_e(\omega_0)|^2}$  exceeds  $\frac{1}{2}$ . Here,  $\omega_0$  is the resonance frequency of the system. The *relative bandwidth* is defined as  $\frac{\Delta\omega}{\omega_0}$  and can be shown to be given by

$$\frac{\Delta\omega}{\omega_0} = \frac{\text{damping}}{\sqrt{\text{stiffness} \times \text{mass}}}. \quad (63)$$

Remember that the resonance period  $T_0$  is given as (cf. (22))

$$T_0 = 2\pi \sqrt{\frac{\text{mass}}{\text{stiffness}}} \quad (64)$$

and that for a WEC oscillating in a single mode, the optimum phase for maximum power absorption happens at resonance. Therefore, in economic terms, we want  $T_0$  to be as large as possible relative to the device size. To do this, according to (64) we can either increase its mass or decrease its stiffness. However, as seen from (63), increasing the mass also reduces the bandwidth, whereas decreasing the stiffness broadens the bandwidth. This means that it is generally a better strategy to decrease the stiffness of the device than to increase its mass.

Geometry (shape and mode of motion) plays an important role, since it influences all three parameters (damping, stiffness, and mass) at the same time. We have looked at this briefly in the example given in Fig. 11. Fig. 18 is another example. Here we have a WEC in the form of a body oscillating along an incline. The bottom plot shows the measured capture width ratio of the device. Changing the angle of the incline changes the power absorption characteristics of the device. Having the incline at  $45^\circ$  to horizontal is seen to be optimal. The broadening of the bandwidth arises from a combination of both a reduction in the hydrostatic stiffness and a variation in the radiation damping and added mass of the body as the inclination angle is varied.

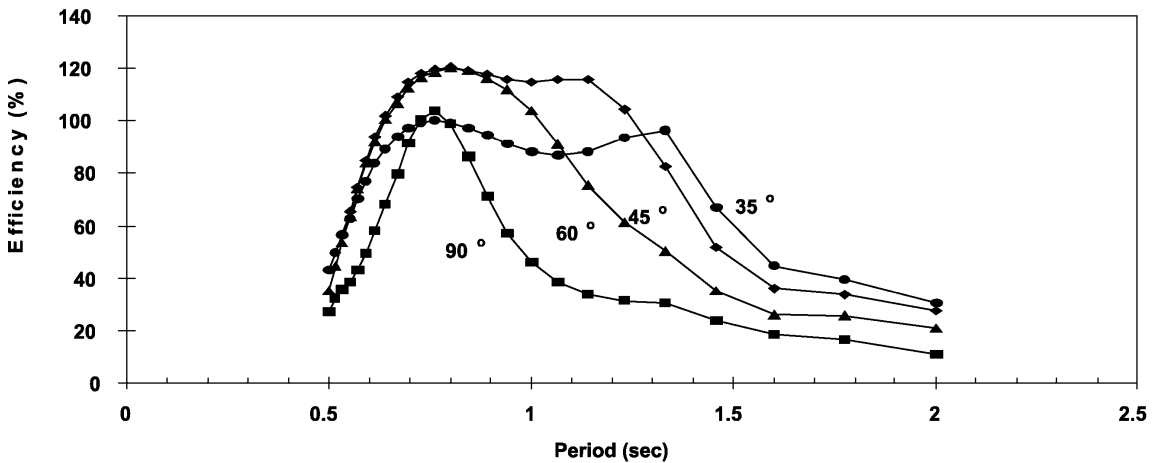
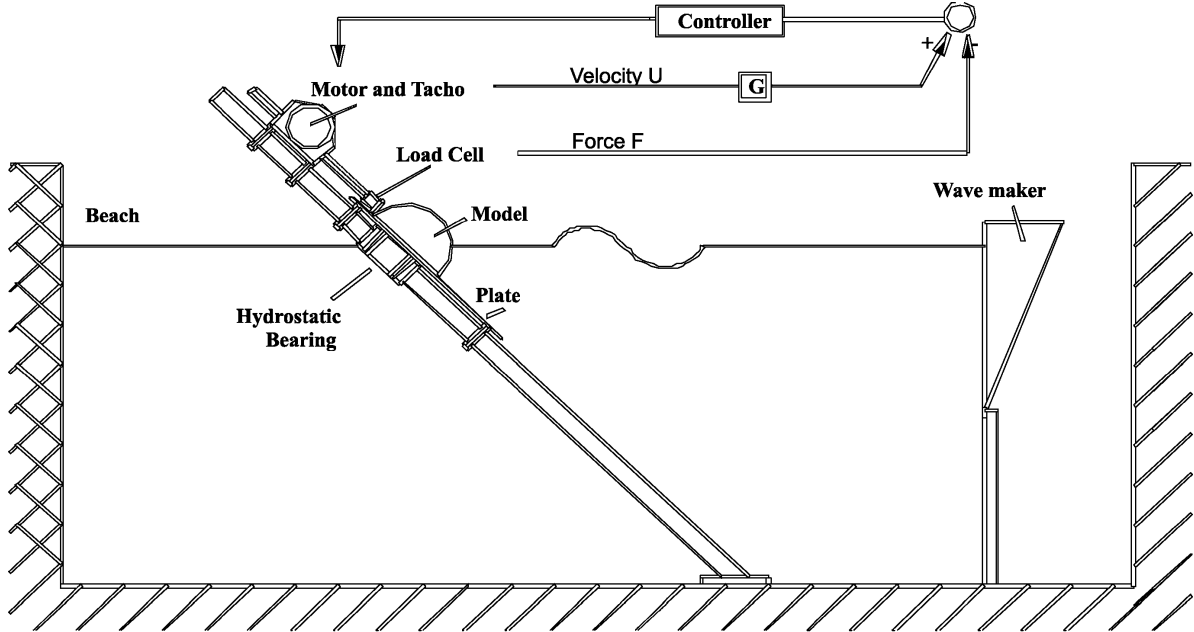


FIGURE 18: Example of how resonance bandwidth is dependent on geometry (the angle of the incline along which the body is oscillating). Vertical motion corresponds to  $90^\circ$ . Reproduced from [10].

#### 4.5 Budal's upper bound

Before concluding this section, let us consider the limitation to the absorbed power arising from the physical constraints of the device. For example, if the body is connected to a piston for power take off, this piston may have a stroke limit. It is then impossible for the body to move beyond this limit. If the optimum displacement required for maximum power absorption exceeds this constraint, it will not be possible to achieve that maximum. There is an upper bound to the absorbed power associated with the finite displacement stroke of the device.

Recall from (49) and (50) that the absorbed power can be written as

$$\begin{aligned}
 P_a &= P_e - P_r \\
 &= \frac{1}{2} |\hat{F}_e| |\hat{u}| \cos \gamma - \frac{1}{2} R_r |\hat{u}|^2.
 \end{aligned} \tag{65}$$

Since  $\cos \gamma \leq 1$  and the radiated power  $P_r = \frac{1}{2}R_r|\hat{u}|^2$  cannot be negative, we have

$$P_a < \frac{1}{2}|\hat{F}_e||\hat{u}|. \quad (66)$$

If the displacement amplitude is limited such that it cannot be greater than  $|\hat{s}_{\max}|$ , we have

$$|\hat{u}| < \omega|\hat{s}_{\max}|. \quad (67)$$

Let us consider a heaving vertical cylindrical body which intersects the water surface, such that the intersection of the body and the water surface at mean position is defined as the waterplane, with an area  $S_w$  (see Fig. 19).

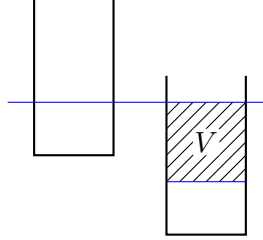


FIGURE 19: The volume stroke of a cylindrical body is equal to the waterplane area times the maximum displacement stroke. The displacement stroke is equal to two times the displacement amplitude.

For this body, it is known that

$$|\hat{F}_e| < \rho g S_w |A|, \quad (68)$$

where  $A$  is the (complex) incident wave amplitude. Further, the maximum displacement limit can be written as

$$|\hat{s}_{\max}| = V/(2S_w), \quad (69)$$

where  $V$  is the volume stroke (see Fig. 19). Therefore, substituting (67)–(69) into (66) gives

$$P_a < \frac{\rho g \omega |A|}{4} V = \frac{\pi \rho g H}{4T} V. \quad (70)$$

This result was first derived by Budal.

There are therefore two upper bounds to the absorbed power of a WEC. The first,  $P_A$ , is the upper bound due to optimal wave interference, assuming the WEC can realise the required optimum motion. The general form is (cf. 56)

$$P_a < P_A = P_{a,\text{MAX}} = \frac{J}{k} G, \quad (71)$$

where  $G$  is the optimum gain function, specific for the WEC or the WEC array. For a monopole radiator, such as an axisymmetric heaving WEC, in deep water,

$$P_a < P_A = \frac{\lambda}{2\pi} J = \frac{\rho g^3 T^3 H^2}{128\pi^3}, \quad (72)$$

where we have used the exact expression of  $J$  and  $\lambda$  for deep-water regular wave (see section 5.2.1 of Part 1).

The second bound,  $P_B$  (the Budal upper bound), is the upper bound due to the physical constraint of the WEC (the WEC has a finite stroke, thus it can displace only a finite volume of water  $V_{\text{water}}$ , which may be less than what is required for optimal wave interference). In general,

$$P_a < P_B \propto |\hat{s}_{\max}| \frac{H}{T} \propto V_{\text{water}} \frac{H}{T}. \quad (73)$$

For a vertical cylindrical WEC moving in heave,

$$P_a < P_B = \frac{\rho g \omega |A|}{4} V = \frac{\pi \rho g H}{4T} V. \quad (74)$$

The two upper bounds,  $P_A$  and  $P_B$ , are plotted in Fig. 20 for a heaving vertical circular cylinder. Because of the physical limitations of the device (a finite stroke length), the theoretical maximum for  $T \gtrsim 8$  s is not realisable.

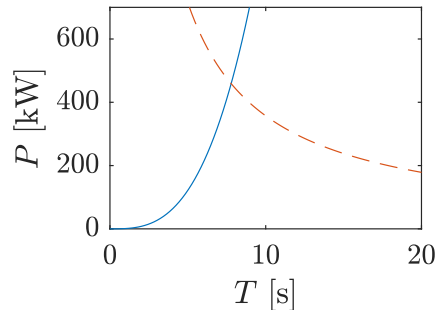


FIGURE 20: Two upper bounds to the power absorbed by a heaving vertical circular cylinder of volume stroke  $V = 226 \text{ m}^3$ . Solid line is  $P_A$ , dashed line is  $P_B$ .

## 5 Physical modelling

Before building an actual WEC in full scale, a WEC developer must have a high level of understanding of how the WEC would respond in a given environmental (wave) condition. Both physical and numerical modelling are critical to provide this understanding. We discuss physical modelling in this section and numerical modelling in the next.

There are a number of reasons for conducting physical model tests: to prove a concept, to validate numerical predictions or theory, or to understand physical problems not predictable otherwise.

What is a physical model? It is a physical system reproduced at a reduced size so that the dominant forces are represented in the model in correct proportion to the prototype. To ensure similitude between prototype and model, the following requirements must be met: *geometric similarity* (ratio between geometrical dimensions), *kinematic similarity* (ratio between motions), *dynamic similarity* (ratio between forces). It is impossible to satisfy all of these for *all* forces, but they must be satisfied for the dominating physics. Violations are called *scale effects*. For WECs, scale effects could arise from air compressibility (relevant for WECs utilising air flow, e.g. for oscillating water columns and pneumatic devices), viscosity, or friction.

For water wave problems, which are relevant for WECs, the governing forces are usually gravity and inertia. Taking the ratio between the two, we have

$$\frac{F_{\text{inertia}}}{F_{\text{gravity}}} \propto \frac{ma}{mg} = \frac{\rho \frac{du}{dt} L^3}{\rho g L^3} = \frac{\rho \frac{du}{dx} \frac{dx}{dt} L^3}{\rho g L^3} = \frac{u^2 L^2}{gL^3} = \frac{u^2}{gL}. \quad (75)$$

Upon taking the square root, we obtain the Froude number

$$\text{Froude number} \equiv \frac{u}{\sqrt{gL}}, \quad (76)$$

which will have to be satisfied at model scale as at prototype (full) scale. The scale factors for quantities of interest can be obtained by equating the Froude number for model and prototype scales. The results are shown in Table 1.

TABLE 1: Scale factors for Froude scaling, reproduced from [4]. Note that  $\lambda$  is used in the table to denote the length scale (not the wavelength), i.e.  $\lambda \equiv L_p/L_m$ .

Characteristic	Dimension	Froude
<b>Geometric</b>		
<b>Length</b>	[L]	$\lambda$
<b>Area</b>	[L <sup>2</sup> ]	$\lambda^2$
<b>Volume</b>	[L <sup>3</sup> ]	$\lambda^3$
<b>Rotation</b>	[L <sup>0</sup> ]	—
<b>Kinematic</b>		
<b>Time</b>	[T]	$\sqrt{\lambda}$
<b>Velocity</b>	[LT <sup>-1</sup> ]	$\sqrt{\lambda}$
<b>Acceleration</b>	[LT <sup>-2</sup> ]	—
<b>Volume Flow</b>	[L <sup>3</sup> T <sup>-1</sup> ]	$\lambda^{5/2}$
<b>Dynamic</b>		
<b>Mass</b>	[M]	$\lambda^3$
<b>Force</b>	[MLT <sup>-2</sup> ]	$\lambda^3$
<b>Pressure</b>	[ML <sup>-1</sup> T <sup>-2</sup> ]	$\lambda$
<b>Power</b>	[ML <sup>2</sup> T <sup>-3</sup> ]	$\lambda^{7/2}$

In model tests of WECs, we are normally interested in measuring the free-surface elevations around the model, water pressures on the body (or air pressure in the case of OWCs and pneumatic devices), forces (power take-off forces, mooring forces, wave excitation and radiation forces), motions (displacement, velocity, acceleration) of the body, flow (air flow in the case of OWCs and other devices utilising air flows, or water flow in the case of overtopping devices), and the absorbed power. It is therefore important to know the Froude scaling factors for these quantities.

Model tests of WECs may be carried out in a wave flume or a wave basin/tank. A wave flume is long and narrow and thus more suited for studying two-dimensional problems. An example is the [UWA wave flume](#). Having a single body at the centre of a flume is equivalent to having a row of infinite number of bodies, since the side walls act as reflectors (or mirrors). A single WEC in a flume therefore represents a long array of WECs. A wave basin/tank, on the other hand, has

comparable length and width and is therefore suited for studying three-dimensional problems such as the interactions of waves with a single WEC in the open sea. An example is the [Plymouth University's wave basin](#). A wave basin of course can never be an exact replica of the open sea, due to the presence of wave reflections from the boundaries. To minimise reflections, both wave flumes and basins normally have a dissipating beach at the opposite end of the wavemaker, whereas the wavemaker normally has an active absorption system (this works using essentially the same principle as the wave absorbing wall in Fig. 13). Piston or hinged paddles are usually employed as the wavemaker. Piston paddles are generally suited for shallow water, while hinged paddles are suited for deep water. The paddles can be programmed to generate different kinds of waves. A wave basin usually has multiple paddles, allowing the generation of oblique and multidirectional waves. The [FloWave](#) wave basin has a circular plan with multiple paddles all around it, allowing it to generate other types of waves not possible to generate in a rectangular basin.

The different types of tests normally conducted in model tests of WECs include

- *Decay tests.* The model is displaced from its mean position and released in otherwise calm water. The natural period of the response is obtained from the recorded motion and the amount of damping is estimated from the decay rate of the response.
- *Forced oscillation tests.* An actuator is used to drive the model in otherwise calm water. The radiation force (added mass and radiation damping) can be obtained.
- *Diffraction tests.* The model is fixed (restrained from moving) and subjected to incident waves. The excitation force can be obtained.
- *Regular wave tests.* The model is subjected to incident regular waves of various periods and amplitudes, with various PTO setting. The frequency response function of quantities of interest, such as displacements and forces, can be obtained. An example is shown in Fig. 21.
- *Irregular wave tests.* These are conducted to replicate a real irregular sea state.
- *Survival tests.* These are conducted to study the response of the WEC in extreme conditions. The model is subjected to a steep irregular sea state or a focused wave group.
- Combinations of the above.

**Example** A WEC is designed to resonate at 8 seconds, where it is expected to generate 100 kW of power. The target deployment location has a water depth of 20 m. If the WEC is to be tested in a wave basin with a water depth of 0.8 m, what would be a suitable model scale to use? At this scale, what would be the resonance period and the expected power output?

**Answer** Using the water depth to decide on the model scale, we have  $0.8 : 20 = 1 : 25$ . According to Froude similitude (Fig. 1), power scales as  $L^{3.5}$ , where  $L$  is the length scale, whereas period (time) scales as  $\sqrt{L}$ . Thus, the model will have a resonance period of  $8/\sqrt{25} = 1.6$  s and produce  $10^5/25^{3.5} = 1.28$  W.

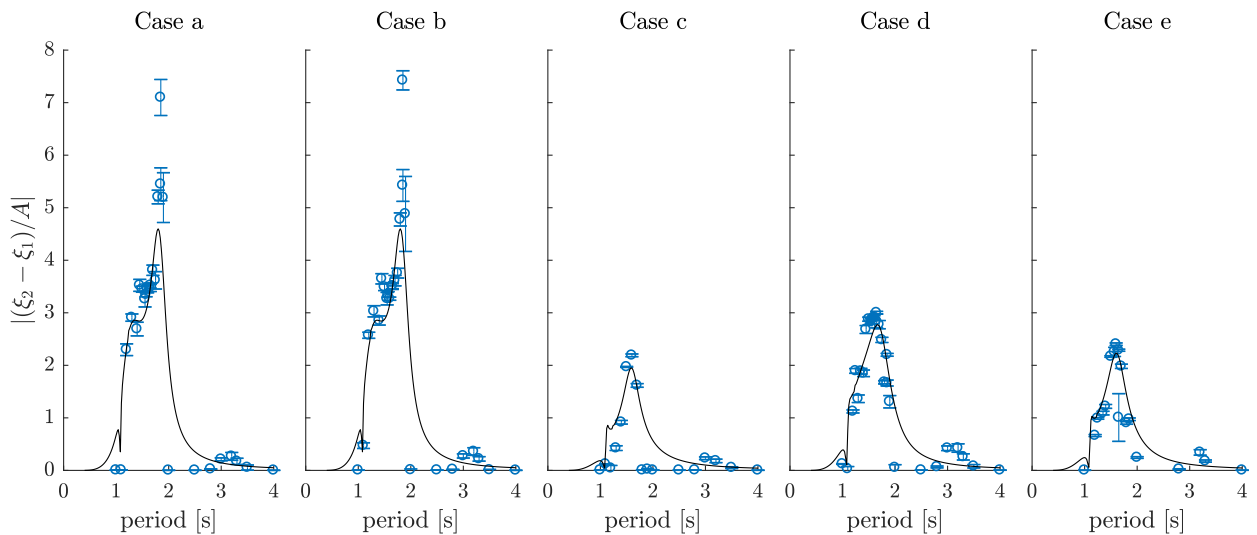
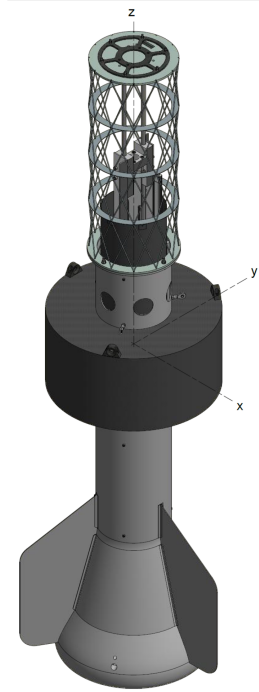
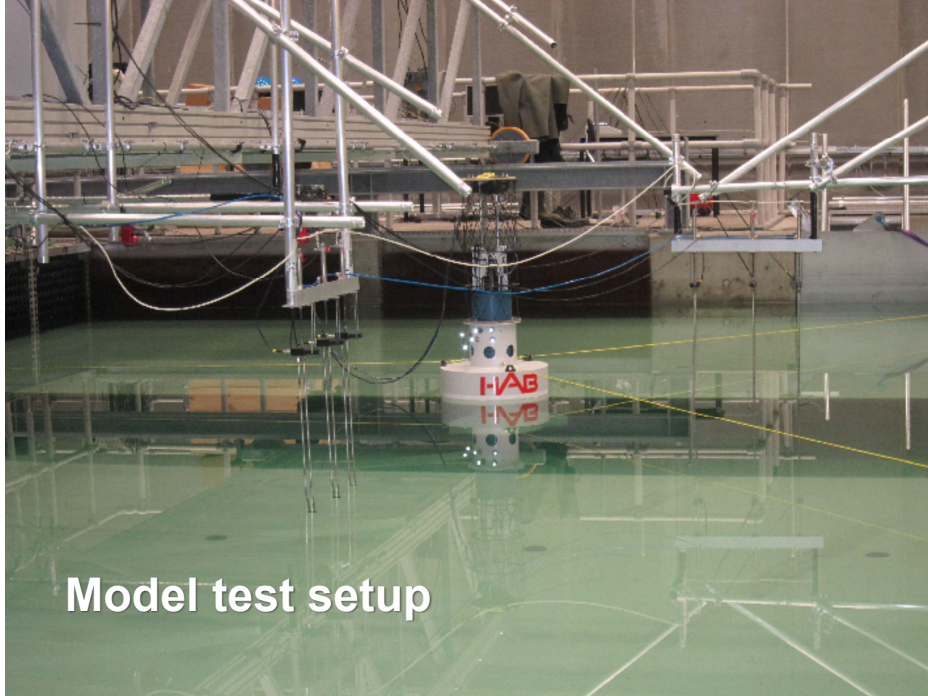


FIGURE 21: A scaled model of a WEC in a wave basin and its technical drawing. The WEC is a heaving device composed of an inner body and an outer body. Power is absorbed through relative motion between the two bodies. Plots at the bottom show comparison of the measured relative displacement between the bodies (points) and the numerical predictions (lines), from [9].

## 6 Numerical modelling

### 6.1 Frequency-domain models

There exists a spectrum of numerical modelling techniques to model a WEC, depending on the level of fidelity and computational efficiency. In the low-fidelity and high-efficiency end of the spectrum is the linear frequency-domain model.

In a frequency-domain model, the equation of motion of the WEC is expressed in the frequency domain. For a WEC oscillating in one mode (a single oscillator), this is just the equation we have considered before (see Section 2.3):

$$\hat{F}_e(\omega) = \{R_m + R_r(\omega) + i\omega [m_m + m_r(\omega) - S_m\omega^{-2}]\} \hat{u}(\omega), \quad (77)$$

As we have seen before, this equation can be solved for the complex velocity amplitude  $\hat{u}(\omega)$ , from which other quantities such as the absorbed power can be calculated. For a WEC oscillating in more than one mode or for an array of multiple WECs, the equation becomes a system of linear equations, but the general form is the same.

A frequency-domain model can be evaluated almost instantly by a computer and is usually the first approach to use. Because it is a linear model, it is necessary to assume the PTO force as linear. Losses can be modelled as a linear damping term. The hydrodynamic problem is solved based on linear potential theory. This generally gives a good approximation. Boundary element method (as implemented in e.g. **WAMIT**, **HydroStar**, **NEMOH**) is commonly used to evaluate the hydrodynamic coefficients (excitation force, added mass, and radiation damping). This requires a panel model of the submerged body geometry. An example is shown in Fig. 22. The figure also shows time histories of the absorbed power calculated from a frequency-domain model.

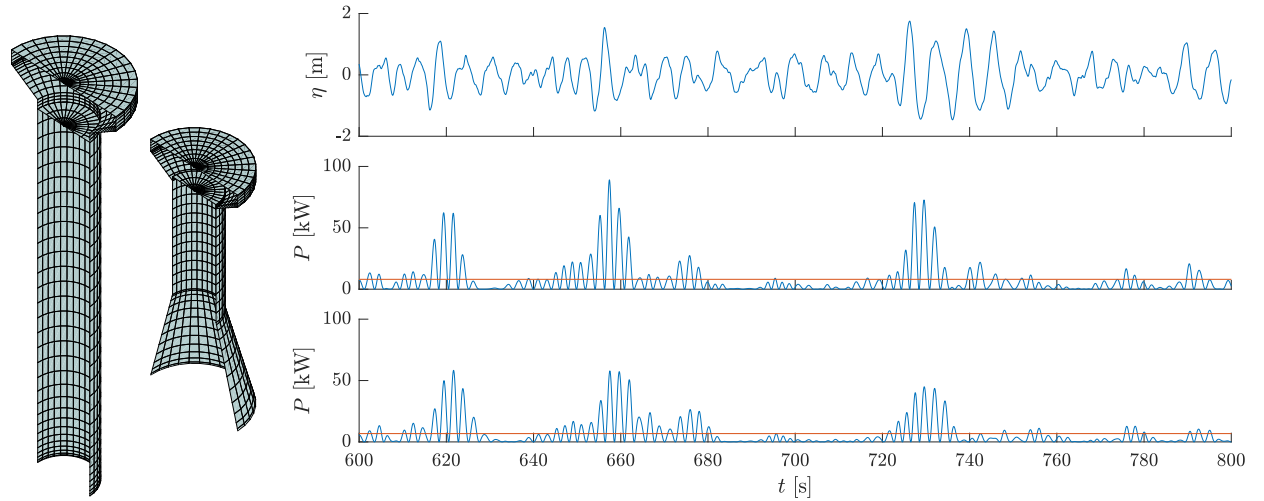


FIGURE 22: Plots on the right show the absorbed power of the two geometric variations of the WEC in Fig. 21, for the same incident irregular waves (plotted at the top). Results were obtained from a frequency-domain model. On the left are the panel models used for computing the hydrodynamic coefficients.

Due to its very low computational cost, a validated frequency-domain model is useful for design optimisation, as this requires numerous computations to be made on possible variations of the design.

## 6.2 Time-domain models

### 6.2.1 Weakly-nonlinear time-domain model

The next step from (linear) frequency-domain models is weakly-nonlinear time-domain models. For a single oscillator, it has the following form:

$$F_e(t) = [m_m + m_r(\infty)]\dot{u}(t) + k(t) * u(t) + S_m s(t) + F_{\text{ext}}(s(t), u(t), t). \quad (78)$$

This time-domain equation (a.k.a. the Cummins' equation) is obtained by taking the inverse Fourier transform of the frequency-domain equation (77). Because of the frequency-dependence of the added mass  $m_r(\omega)$  and radiation damping  $R_r(\omega)$ , the wave radiation force contains a convolution term  $k(t) * u(t) = \int_0^t k(\tau)u(t - \tau)d\tau$ , where  $k(t) = \frac{2}{\pi} \int_0^\infty R_r(\omega) \cos(\omega t)d\omega$  is the radiation *impulse response function*. The convolution term is a memory term, related to the fact that waves radiated by the body in the past continue to be felt by the body at present. The other part of the radiation force is the term containing  $m_r(\infty)$ , the infinite-frequency added mass. In equation (78),  $s(t)$  is the body displacement.

As in a frequency-domain model, the hydrodynamic forces are typically assumed linear. However, the time-domain formulation makes it possible to include other nonlinearities, such as nonlinear PTO forces, drag, control forces, and nonlinear restoring forces. These are all contained in  $F_{\text{ext}}(s(t), u(t), t)$ , which is a general nonlinear force that includes the PTO force. Instead of a linear damping term, the PTO force can be modelled more realistically with a time-domain model. An example simulation result from a time-domain model is shown in Fig. 23. In this example, a hydraulic system is used for the PTO. A detailed model of the hydraulic PTO involving nonlinear terms is included in the time-domain model.

Time-domain models such as (78) are usually solved numerically using a time-stepping scheme, such as the Runge-Kutta methods. The convolution term, which is an integral from time past to the present, needs to be recalculated at every time step and can be time-consuming to compute. However, it is possible to speed up computation by replacing the convolution with some approximations.

### 6.2.2 Fully-nonlinear time-domain models

The preceding models (frequency-domain models and weakly-nonlinear time-domain models) are commonly used because they are computationally cheap. For WECs, we are mainly interested in the performance (power output) of the device in small to moderate wave steepness (which happen most of the time), and these models generally give reasonably good predictions in these cases. They are also useful for parametric studies or design optimisation studies, as the effect of different design parameters on the device performance can be evaluated relatively quickly.

However, understanding certain aspects of the wave-structure interaction problems may require the use of higher-fidelity models, which can reproduce the physics of the problem more accurately at the expense of much higher computational costs. Commonly used nonlinear time-domain models include fully-nonlinear potential flow models, which are suitable for steep but non-breaking waves, and a range of higher-fidelity computational fluid dynamics (CFD) models, which can capture breaking waves and account for flow separation.

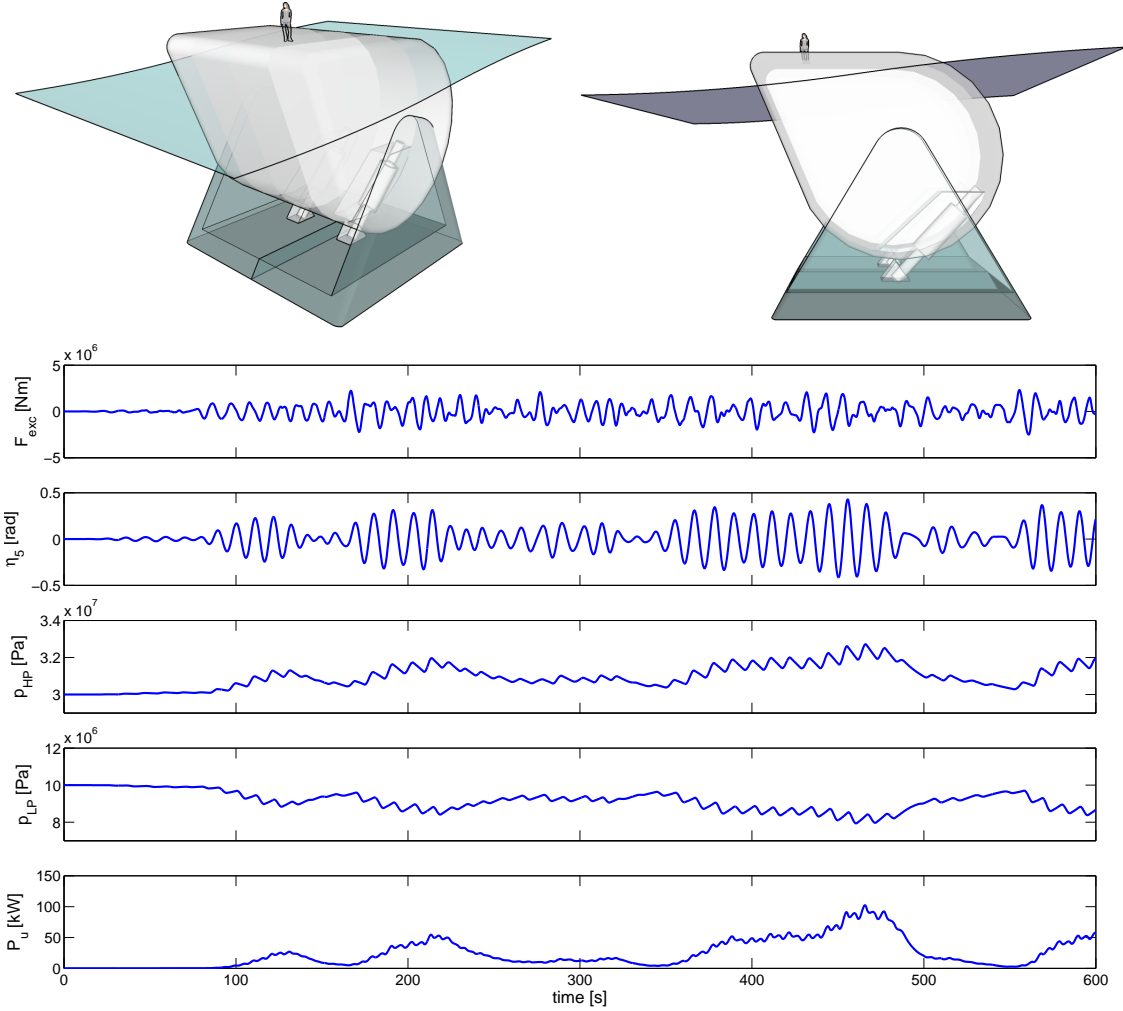


FIGURE 23: A seabed-mounted WEC similar to the Salter Duck, reproduced from [7]. The device is connected to a hydraulic PTO system. The plots show the response of the device, including the angular displacement, pressures in the high- and low-pressure accumulators, and power output, under irregular wave excitations. Results were obtained from a time-domain model.

### 6.3 Modelling oscillating water column

Before concluding this section, let us say a few words about modelling of oscillating water column (OWC) devices. To model an OWC in the frequency domain, two approaches are possible: the massless piston model [1] and the pressure distribution model [2]. The massless piston model approximates the top surface of the water column as a massless rigid piston. Thus the models for oscillating-body WECs as given by (77) and (78) are applicable. Because the rigid piston remains horizontal at all times, this approximate model works well as long as the size of the water column is small in comparison with the wavelength, but becomes less valid for shorter wavelengths. In the pressure distribution model, no such approximation is necessary and so it is more accurate. The radiation problem is described by quantities analogous to added mass and radiation damping, but instead of force and body velocity these quantities relate dynamic air pressure and volume flow.

## 7 Mean power output in irregular sea

In Part 1, we discussed how to calculate the mean wave-power level at a given site, when the long-term distribution of wave heights and periods at the site is available. The mean power output of a WEC can be calculated in a similar way.

The mean power output from a given sea state characterised by a spectrum  $S(\omega)$  is

$$P_a(H_s, T_p) = 2 \int_0^\infty \frac{P_a(\omega)}{|A|^2} S(\omega) d\omega, \quad (79)$$

where  $\frac{P_a(\omega)}{|A|^2}$  is the so-called *power function* (remember that  $A$  is the incident wave amplitude). Alternatively, if the capture width  $d_a$  (as a function of frequency) is known, then

$$P_a(H_s, T_p) = \rho g \int_0^\infty d_a v_g S(\omega) d\omega. \quad (80)$$

A table of the mean power output  $P_a(H_s, T_p)$  for different combinations of  $H_s$  and  $T_p$  is often called the *power matrix*.

The mean power output from a wave climate, given the scatter diagram (joint probability table of wave heights and periods) at a given site, can be calculated in the same way as the mean wave-power level  $\bar{J}$  is calculated:

$$\bar{P} = \sum_{H_s} \sum_{T_p} P_a(H_s, T_p) C(H_s, T_p), \quad (81)$$

where  $\sum_{H_s} \sum_{T_p} C(H_s, T_p) = 1$  (see Part 1).

The mean capture width for the entire wave climate can then be obtained as

$$\bar{d}_a = \frac{\bar{P}}{\bar{J}}. \quad (82)$$

## 8 Useful and interesting links

- **National Map**

The National Map has resource maps for renewable energy in Australia, including wind, hydro, wave, and tidal. For wave, click on ‘Explore map data’, and go to Energy > Renewable Energy > Marine > Australian Marine Energy Atlas > Marine Energy Context Layers > Wave Energy Resource, where you will find different options, including ‘Wave Energy Flux’, which is the wave-power level.

- **European Marine Energy Centre (EMEC)**

The European Marine Energy Centre, established in 2003, is the world’s first and leading facility for demonstrating and testing wave and tidal energy converters. Check out the wave energy converters that have been tested there—also relevant for tidal. They also publish a set of standards and guidelines for the marine energy industry, covering a lot of aspects, from resource assessment to grid connection.

- **Wave Energy Scotland (WES)**

Wave Energy Scotland is a technology development body set up by the Scottish Government to facilitate the development of wave energy in Scotland. It implements a phase-gate approach to ensure that only the most promising technologies receive maximum investment. This model has now been adopted in the EuropeWave R&D programme of the European Union.

- **Wave Energy Programme — Edinburgh Research Archive**

Archives from the Edinburgh Wave Power Project and the UK Department of Energy - Wave Energy Programme (1974–1983). The Wave Power Group at the University of Edinburgh dates back to 1974—the year that Stephen Salter invented the ‘Duck’.

- **Johannes Falnes’ Homepage**

Johannes Falnes, along with Stephen Salter, is a living legend for his pioneering research on wave energy. His website contains a historical account of early wave energy research, from a Norwegian perspective.

## References

- [1] D. V. Evans. The oscillating water column wave-energy device. *J. Inst. Maths Applics.*, 22:423–433, 1978.
- [2] D. V. Evans. Wave-power absorption by systems of oscillating surface pressure distributions. *Journal of Fluid Mechanics*, 114:481–499, 1982.
- [3] Johannes Falnes and Adi Kurniawan. *Ocean Waves and Oscillating Systems: Linear Interactions Including Wave-Energy Extraction*, volume 8 of *Cambridge Ocean Technology Series*. Cambridge University Press, 2 edition, 2020.
- [4] B. Holmes. *Tank testing of wave energy conversion systems*. The European Marine Energy Centre, Orkney, UK, 2009.
- [5] J. M. J. Journée and W. W. Massie. *Offshore Hydromechanics*. Delft University of Technology, 2001. Available from <http://www.shipmotions.nl/DUT/LectureNotes/OffshoreHydromechanics.pdf>.
- [6] A. Kurniawan, J. Hals, and T. Moan. Assessment of time-domain models of wave energy conversion systems. In *Proceedings of the 9th European Wave and Tidal Energy Conference*, Southampton, 2011.
- [7] A. Kurniawan, E. Pedersen, and T. Moan. Bond graph modelling of a wave energy conversion system with hydraulic power take-off. *Renewable Energy*, 38(1):234–244, 2012.
- [8] Adi Kurniawan. *Modelling and geometry optimisation of wave energy converters*. PhD thesis, Norges teknisk-naturvitenskapelige universitet, 2013.

- [9] Adi Kurniawan, Matthias Grassow, and Francesco Ferri. Numerical modelling and wave tank testing of a self-reacting two-body wave energy device. *Ships and Offshore Structures*, 14(sup1):344–356, 2019.
- [10] S. H. Salter. Looking back. In J. Cruz, editor, *Ocean Wave Energy: Current Status and Future Perspectives*. Springer, 2008.
- [11] WAMIT. *User Manual*. WAMIT, Inc., Chestnut Hill, MA, 2016. Version 7.2.

